Two Dimensional Analysis of Faraday Type Linear Diverging Combustion Gas MHD Generator

By

Takehisa HARA*, Nobuhiko HAYANOSE** and Jūrō UMOTO*

(Received March 31, 1976)

Abstract

In this paper the authors investigate the effects of non-equilibrium ionization in the cool gasdynamic boundary layer in a combustion gas MHD generator. A two dimensional analysis is applied to the linear diverging Faraday type channel, and predicts that the current concentrates near the electrode edges and Hall current in the core is positive in the case neglecting the boundary layer. However, the current consentration is almost diminished and the Hall current in the core becomes negative in the case considering the effect of nonequilibrium ionization in the cold boundary layer. Also, it is clarified that at the condition of wall temperature $T_w=1500\ K$, the generator output power in a nonequilibrium case is about ten times larger than that in an equilibrium case.

Apparent conductivity, apparent Hall parameter, power density, and local conversion efficiency are calculated and detailed discussions on these quantities are made.

1. Introduction

The boundary layer rising in an MHD channel decreases the power output, efficiency, etc. of the generator. Especially in the thermal equilibrium combustion MHD generator, in which both electron and gas temperatures are nearly equal, it is thought that the deterioration of the generator characteristics due to the layer is large[1),2)]. However, since actually the electron temperature elevates above the gas temperature in the boundary layer by the existence of nonequilibrium ionization, it is expected that the generator power output doesn't degrade so much as usually thought. Moreover, the presence of a boundary layer relaxes the current concentration rising at the electrode ends of the generator[3)].

In this paper, the authors describe a two dimensional computer model for the Faraday type combustion gas MHD generator channel, where electron temperature elevation in the boundary layer is considered. They investigate the effect of boundary

* Department of Electrical Engineering
** Department of Electrical Engineering. Present address: Kobe Technical College

layer and wall temperatures upon the generator characteristics and the current distribution. Moreover, in order to analyze the performance characteristics of a linear diverging channel, which is ordinarily constructed, the authors introduce the cylindrical coordinate system.

2. Basic Equations

2.1 Basic Equations in Cylindrical Coordinate System

Let us consider the cylindrical coordinate system with the axis denoted as r, θ and z. A strong magnetic field $\boldsymbol{B}=(0, 0, B)$ is imposed parallel with z axis, and its positive direction (See Fig. 1). In the r, θ plane normal to $\boldsymbol{B}$, the working fluid flows steadily with velocity $\boldsymbol{U}=(U, 0, 0,)$ and a conduction current density $\boldsymbol{J}$ is established. If the magnetic Reynolds number of the flow is small, the appropriate equations for the electric field $\boldsymbol{E}=(E_r, E_\theta, 0)$ and the current density $\boldsymbol{J}=(J_r, J_\theta, 0)$ are the steady-state Maxwell's equation and the current conservation equation for an electrically neutral fluid, namely

$$\text{curl } \boldsymbol{E} = 0, \qquad \text{div } \boldsymbol{J} = 0 \tag{1}$$

The generalized Ohm's law is

$$\left.\begin{aligned} \boldsymbol{J} &= \sigma \boldsymbol{E}^* - \beta(\boldsymbol{J}\times\boldsymbol{B})/B \\ \boldsymbol{E}^* &= \boldsymbol{E} + \boldsymbol{u}\times\boldsymbol{B} \end{aligned}\right\} \tag{2}$$

in which σ is the scalar conductivity and β is the Hall parameter. From Eq. (1),

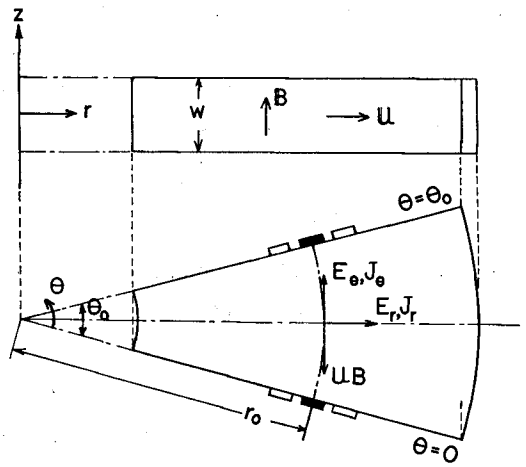

Fig. 1. Coordinate system and configuration of linear diverging generator channel.

the current J may be represented by the stream function

$$J_r = \frac{1}{r}\frac{\partial \Psi}{\partial \theta}, \qquad J_\theta = -\frac{\partial \Psi}{\partial r} \tag{3}$$

Then we obtain the differential equation for Ψ as follows:

$$r\frac{\partial^2 \Psi}{\partial r^2}+\frac{1}{r}\frac{\partial^2 \Psi}{\partial \theta^2}+\frac{\partial \Psi}{\partial r}+P(r,\theta)\frac{\partial \Psi}{\partial r}+Q(r,\theta)\frac{\partial \Psi}{\partial \theta} = R(r,\theta) \tag{4}$$

where

$$\left.\begin{aligned} P(r,\theta) &= \sigma\left\{r\frac{\partial}{\partial r}\left(\frac{1}{\sigma}\right)-\frac{\partial}{\partial \theta}\left(\frac{\beta}{\sigma}\right)\right\} \\ Q(r,\theta) &= \sigma\left\{\frac{1}{r}\frac{\partial}{\partial r}\left(\frac{1}{\sigma}\right)+\frac{\partial}{\partial r}\left(\frac{\beta}{\sigma}\right)\right\} \\ R(r,\theta) &= \sigma\frac{\partial}{\partial r}(ruB) \end{aligned}\right\} \tag{5}$$

We assume that the conducting surfaces in contact with the gas are infinitely conducting and the insulating surfaces in contact with the gas are infinitely non-conducting. Then we have the following boundary conditions on the electrode and insulator respectively.

$$E_r = 0, \qquad J_\theta = 0 \tag{6}$$

2.2 Application to Linear Diverging Channel

Now let us consider the application of the above basic equations to a two dimensional linear diverging Faraday type channel, with conductors and insulators arranged in an infinitely long periodic structure as shown in Fig. 1. The gas velocity u is assumed to be in the positive r direction and to be a function of θ only. For such a configuration, the boundary conditions on Ψ may be specified as follows. The periodicity of the conductors and insulators requires

$$\begin{aligned} &\Psi(r+s,\theta) = \Psi(r,\theta)+\Delta\Psi \\ &\Delta\Psi = I/w \end{aligned} \tag{7}$$

where I and w are the load current and the channel width along axis respectively. The boundary conditions on Ψ on the conducting and insulating surfaces are obtained as follows:

$$\left.\begin{aligned} &\Psi = 0, && -s/2 < r-r_0 < -c/2, && \theta = 0, \theta_0 \\ &\Psi = \Delta\Psi, && c/2 < r-r_0 < s/2, && \theta = 0, \theta_0 \\ &\frac{1}{r}\frac{\partial \Psi}{\partial \theta}-\beta\frac{\partial \Psi}{\partial r} = 0, && -c/2 < r-r_0 < c/2, && \theta = 0, \theta_0 \end{aligned}\right\} \tag{8}$$

where r_0, θ_0, s and c are the distance between the origin and the center of an electrode, the diverging angle of the channel, the electrode pitch and the electrode width respectively.

3. Scalar Conductivity, Hall Parameter, Electrical Efficiency and Output

3.1 Scalar Conductivity and Hall Parameter

An elevation of the electron temperature and the electron number density above the gas temperature and the corresponding equilibrium number density respectively are nearly always present in the wall-boundary regions, even in so-called "thermal equilibrium ionization" generators (i.e., generators in which the electron temperature is equal to the gas temperature in the core of the flow).

The temperature rise is due to the fact that for a given current density level, the electron temperature elevation is inversely proportional to the square of the electron number density, which is several orders of magnitude lower in the cold boundary layers close to the walls than it is in the core. Here, let us derive the scalar conductivity of the combustion gas plasma in the case of the nonequilibrium condition mentioned above.

Scalar conductivity σ and Hall parameter β are expressed as follows:

$$\sigma = \frac{n_e e^2}{m_e \nu_e}, \qquad \beta = \frac{eB}{m_e \nu_e} \tag{9}$$

where e : electron charge
m_e: mass of an electron
ν_e : collision frequency of electrons
n_e : electron number density

In the case where the ionization process mainly depends on collision between electrons and other particles, the electron number density is approximately determined by the Saha equation as follows:

$$n_e = \sqrt{n_s}\left(\frac{2\pi m_e k}{h^2}\right)^{3/4} T_e^{3/4} \exp\left(-\frac{T_i}{T_e}\right) \tag{10}$$

where n_s : neutral seed atom number density
h : Plank's constant
k : Boltzman's constant
T_i : ionized temperature of seed atom

Next ν_e is expressed as follows:

$$\nu_e = \left(\frac{8k}{\pi m_e}\right)^{1/2} T_e^{1/2} \sum n_j Q_j \tag{11}$$

where n_j and Q_j denote the number density of the j-th particle and collision cross section between electrons and j-th particle.

Substituting Eqs. (10) and (11) into Eq. (9) yields

$$\sigma = \left(\frac{2\pi m_e k}{h^2}\right)^{3/4} \left(\frac{\pi}{8km_e}\right)^{1/2} e^2 \sqrt{n_s} (\sum n_j Q_j)^{-1} T_e^{1/4} \exp\left(-\frac{T_I}{T_e}\right) \tag{12}$$

As we may assume that n_s and $\sum n_j Q_j$ are decided by gas pressure p and temperature T, let us write the following expression

$$\sigma = Cp^m T^n T_e^{1/4} \exp(-T_I/T_e) \tag{13}$$

for the scalar conductivity σ of combustion gas plasma.
Similarly we can write the Hall parameter β as follows:

$$\beta = C' p^{m'} T^{n'} T_e^{-1/2} B \tag{14}$$

T_e in above Eqs. (13) and (14) is decided by the following energy balance equation.

$$\frac{3}{2}\{2\delta R(p,T)\}(T_e - T)\left(\frac{\sigma B}{\beta}\right)^2 = J^2 \tag{15}$$

where δ and $R(p, T)$ are the effective electron energy loss factor of the working gas and gas constant respectively.

Moreover, for thermal equilibrium ionization ($T \fallingdotseq T_e$), Eqs. (13) and (14) reduce to the following equations

$$\sigma = Cp^m T^{n+1/4} \exp(-T_I/T) \tag{16}$$

$$\beta = C' p^{m'} T^{n'-1/2} B \tag{17}$$

respectively.

3.2 Gas Velocity and Temperature

The variations of the gas velocity and temperature in θ direction are prescribed by means of the following expression[4]

$$\frac{u}{u_\infty} = \frac{T - T_w}{T_\infty - T_w} = \left\{4\frac{\theta}{\theta_0}\left(1 - \frac{\theta}{\theta_0}\right)\right\}^{ck} \tag{18}$$

where u_∞ and T_∞ are the gas velocity and temperature in the core respectively, and T_w is the wall temperature. The thickness of the thermal and velocity boundary layers can be adjusted by changing the exponents $ck (0 \leqslant ck \leqslant 1)$.

Moreover, in order to be sure that u is a function of θ only, the following relation

$$\frac{pr}{T} = \text{const} \tag{19}$$

must be satisfied. Here we assume that T varies with -60 k/m along r direction and p is determined to satisfy Eq. (19).

3.3 Electrical Efficiency and Output Power Density

The apparent conductivity and the apparent Hall parameter of the Faraday generator are defined by

$$\left.\begin{aligned} \sigma_{app} &= \langle J_\theta \rangle / \langle E_\theta^* \rangle \\ \beta_{app} &= \langle E_r \rangle / \langle E_\theta^* \rangle \end{aligned}\right\} \tag{20}$$

respectively, where the bracket $\langle \quad \rangle$ means an average in a volume. In the Faraday generator, the local electrical efficiency η is equivalent to the loading factor κ; and they are expressed as follows:

$$\eta = \kappa = \frac{\langle E_y \rangle}{\langle uB \rangle} \tag{21}$$

The averaged output power density is given by

$$P = -\langle E_\theta \rangle \langle J_\theta \rangle = \sigma_{app} \kappa (1-\kappa) \langle uB \rangle^2 \tag{22}$$

4. Numerical Calculations and Discussions

4.1 Numerical Conditions

Numerical calculation is carried out for the linear diverging Faraday generator channel in which a heavy oil is used as the fuel and KOH and K_2SO_4 are seeded so that the potassium atom is contained in a ratio of 1 wt% to the combustion gas. In calculating the conductivity σ and Hall parameter β, we should decide the values of the constants C, m, n, C', m' and n' in Eqs. (13) and (14). These values are chosen so that Eqs. (16) and (17) might give the good approximate expressions for σ and β in the tables[5], which have been obtained in the above mentioned case, as follows:

$$\left.\begin{aligned} &C=89.9, \quad m=-0.51, \quad n=-0.78 \\ &C'=4.43, \quad m'=-0.99, \quad n'=1.47 \\ &T_i=2517 \text{ K} \end{aligned}\right\} \tag{23}$$

Moreover, the gas constant $R(p, T)$ in Eq. (15) is also obtained from the same gas tables as follows:

$$R(p, T) = \begin{cases} 69.2 + 6.41 \times 10^{-10} p^{-0.396} (T - 1800)^{3.24} & T \geqslant 1800 \text{ K}, \\ 69.2 & T < 1800 \text{ K}, \end{cases} \text{ cal/Kg·K} \quad (24)$$

Next, we adopt the following gas dynamic variables and magnetic induction

$$\left.\begin{aligned} & u_\infty = 800 \text{ m/s} \\ & T_\infty|_{r=r_0} = 2500 \text{ K} \\ & p|_{r=r_0} = 3 \text{ atm} \\ & \partial T/\partial r = -60 \text{ K/m} \\ & B = 5 \text{ T} \end{aligned}\right\} \quad (25)$$

We use

$$ck = 1/7 \quad (26)$$

for the configuration of the boundary layer. Finally, we assume each dimension of the channel as follows:

$$\left.\begin{aligned} & h = r_0\theta_0 = 0.5 \text{ m} \\ & w = 0.2 \text{ m} \\ & s = 0.1 \text{ m} \\ & c = 0.08 \text{ m} \\ & \theta_0 = 10° \end{aligned}\right\} \quad (27)$$

where $h = r_0\theta_0$ is the channel hight.

4.2 Results and Discussions

Before we carry out the two-dimensional analysis, we will investigate the effect of nonequilibrium ionization in the gas dynamic boundary layer[6]. Fig. 2 shows the relation of T_e vs. T which is calculated from Eqs. (13), (14) and (15) for $J=1.0$ A/cm^2. Fig. 3 shows σ as a function of J for the cases of $T=1500$ K, 1900 K and 2500 K. These figures demonstrate that the effect of nonequilibrium ionization cannot be negligible in a cold boundary layer region[3].

Next, in Figs. 4 to 6 we plot the current distributions in the channel obtained by the two-dimensional numerical calculation. Fig. 4 illustrates the current distribution in the case where the thermal boundary layer is not considered, namely for $T_w=2500$ K (Case 1). Fig. 5 shows the distribution in the case where it is assumed that non-equilibrium ionization does not occur in the thermal boundary layer for $T_w=1500$ K, namely $\delta=\infty$ (Case 2). Next, Fig. 6 regards the case where the effect of nonequilibrium ionization is taken into consideration for $T_w=1500$ K, namely $\delta=500$ (Case

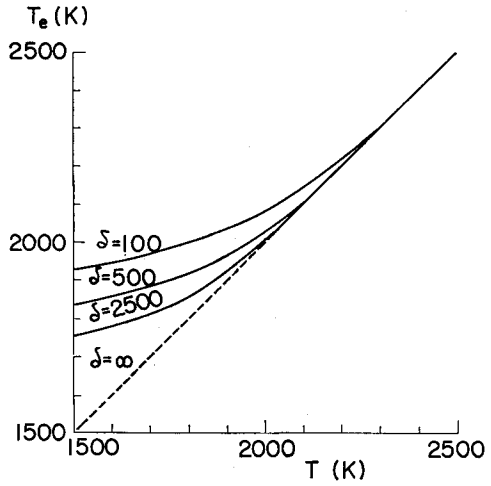

Fig. 2. Electron temperature T vs. gas temperature T_e for $J=1.0$ A/cm^2 and for various δ.

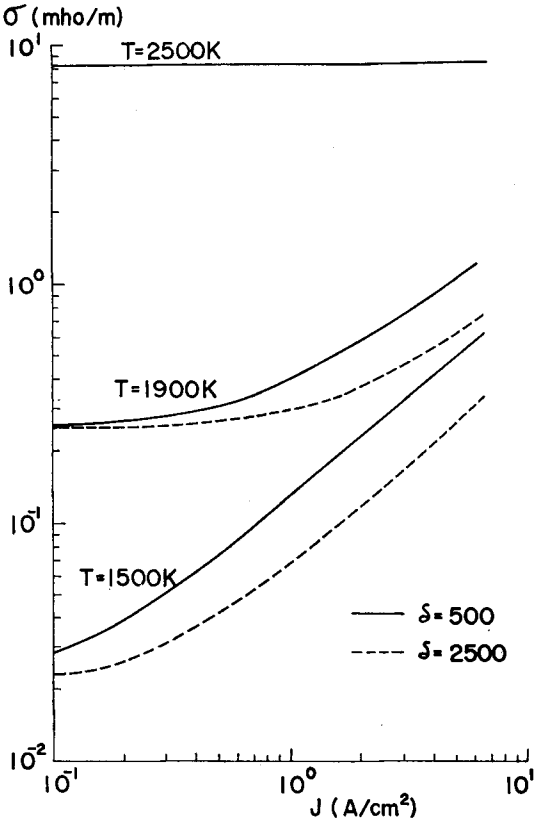

Fig. 3. Scalar conductivity σ vs. current density J for $T=1500$ K, 1900 K and 2500 K.

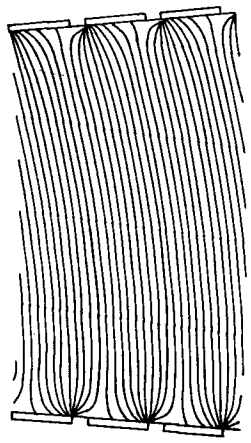

Fig. 4. Current distribution for $T_w=2500$ K and $\delta=\infty$.

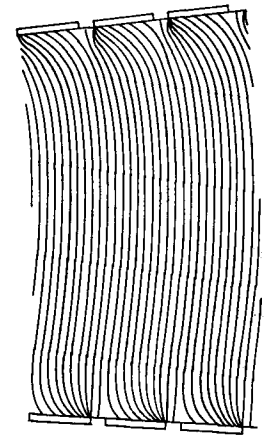

Fig. 5. Current distribution for $T_w=1500$ K and $\delta=\infty$.

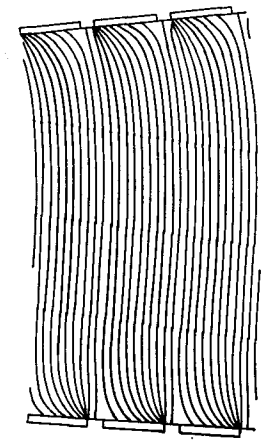

Fig. 6. Current distribution for $T_w=1500$ K and $\delta=500$.

3). From these figures, we see that the direction of the Hall current in the hot wall case (Case 1) is essentially the same as it is in a uniform gas property generator. However, in the cold wall case (Case 2) the direction of the Hall current is reversed. In the cold wall case considering nonequilibrium ionization (Case 3), the current distribution is almost the same as it is in Case 2, exept that in Case 3 current concentration on the electrode occurs slightly more than in Case 2. Moreover, in Cases 2 and 3, since $\langle J_r \rangle$ is nearly equal zero, we need not take the conductivity reduction by finite segmentation into consideration.

Fig. 7 (a), (b) and (c) show the relations of P, normalized apparent conductivity $\sigma_{app}/\sigma_\infty$, where σ_∞ is the conductivity in the gas core, and the normalized apparent Hall parameter β_{app}/β_∞, where β_∞ is the Hall parameter in the core, vs. the wall temperature T_w respectively, for $\kappa=0.5$ and $\delta=500$, 2500 and ∞. In the case of $\delta=500$, $P=5.2$, 13.4 and 25.0 MW/m^3 for $T_w=1500$, 1900 and 2500 K respectively. However, in the case of $\delta=\infty$, P decreases to 0.68, 11.0 and 25.0 MW/m^3 for $T_w=1500$, 1900 and 2500 K respectively. Namely, in a case considering the effect of nonequilibrium ionization, the power density is about 10 and 1.2 times as large as that in a case not considering that effect for $T_w=1500$ and 1900 K respectively. Moreover, it is seen that the relations of σ_{app} and β_{app} vs. T_w are approximately similar to the relation of P vs. T_w. From the above results, it is evident that we should use the two-temperature model considering the effect of nonequilibrium ionization in the boundary layer.

Fig. 8 illustrates P, $\sigma_{app}/\sigma_\infty$, β_{app}/β_∞, η and the average Faraday current density

$\langle J_\theta \rangle$ as a function of κ. Also, from the figure we see that the maximum output power density is obtained for $\kappa<0.5$, while it is got for $\kappa=0.5$ in the generator of the uniform gas. In this connection, as shown in Fig. 8, the generator generates a maximum power density 5.8 MW/m^3 for $\kappa=0.35$.

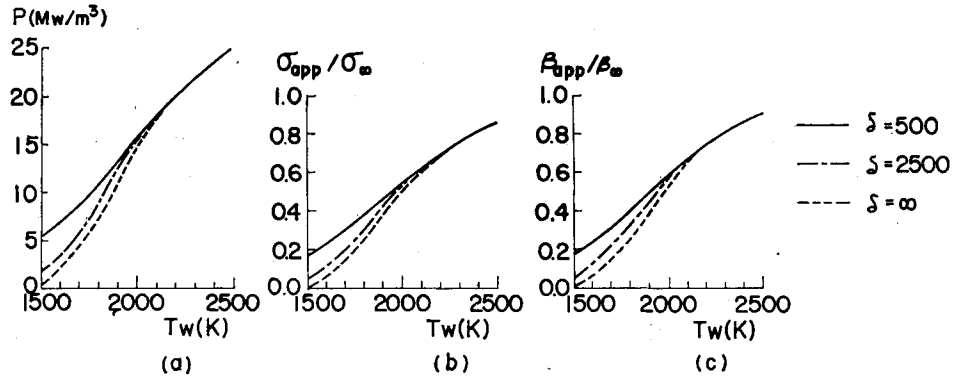

Fig. 7. Output power density P, nolmalized apparent conductivity $\sigma_{app}/\sigma_\infty$ and nolmalized apparent Hall parameter β_{app}/β_∞.
(a) Output power density P vs. wall temperature T_w.
(b) Nolmalized apparent conductivity $\sigma_{app}/\sigma_\infty$ vs. wall temperature T_w.
(c) Nolmalized apparent Hall parameter β_{app}/β_∞ vs. wall temperature T_w.

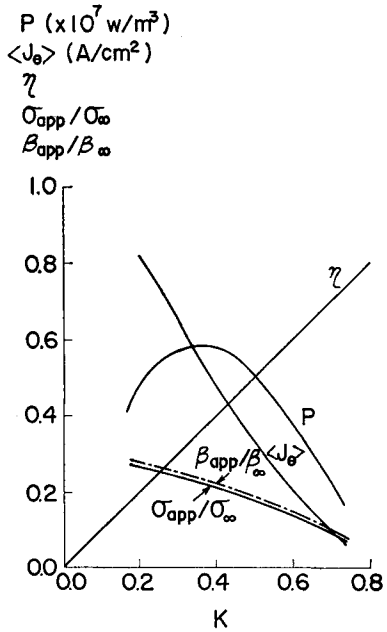

Fig. 8. Values of P, $\sigma_{app}/\sigma_\infty$, β_{app}/β_∞, η and $\langle J_\theta \rangle$ vs. loading factor κ.

5. Conclusion

The preceding chapters have presented a two-dimensional analysis of a linear diverging Faraday type combustion MHD generator channel. In Section 2, the partial differential equation for current stream function Ψ in a linear diverging channel was introduced. Then, in Section 3, the calculating method of scalar conductivity and the Hall parameter in a combustion generator considering the nonequilibrium ionization effect in the cold boundary region was shown.

Next, in Section 4, it was shown that although the current distribution in a case considering the effect of nonequilibrium ionization in the boundary layer is almost same as the distribution in a case not considering that effect, the output power in the former case become much larger than that in the latter case. So, it is evident that even in a combustion generator, the two-temperature model considering the effect of nonequilibrium ionization in the boundary layer should be used.

Finally, it was made clear that the maximum output power is obtained for $\kappa=\eta<0.5$ in the cold wall type generator.

References

1) D. A. Oliver; AIAA J., **5**, No. 8, 1424 (1967).
2) Y. C. L. Wu; Proc. of 10th Symp. on Eng. Aspects of MHD, 23 (1969).
3) S. T. Demetriades; Proc. of 12th Symp. on Eng. Aspects of MHD, I. 5 (1972).
4) L. L. Lengel; Energy Conversion, **9**, 13 (1969).
5) Technical Report of the Investigation Committee of MHD Generator Plant (1973).
6) G. S. Argyropoulos; Proc. of 13th Symp. on Eng. Aspects of MHD, VII 6 (1973).